Fuel 221 (2018) 417–424

Contents lists available at ScienceDirect

Fuel

journal homepage: www.elsevier.com/locate/fuel

Full Length Article

A Preliminary investigation of CO effects on lignite liquefaction process

Huan Li[a,b], Shiyong Wu[a,b,*], Youqing Wu[a,b,*], Sheng Huang[a,b], Jinsheng Gao[a,b]

[a] Department of Chemical Engineering for Energy Resources, School of Resources and Environmental Engineering, East China University of Science and Technology, Shanghai 200237, China

[b] Key Laboratory of Coal Gasification and Energy Chemical Engineering of Ministry of Education, East China University of Science and Technology, Shanghai 200237, China

ARTICLE INFO

Keywords:
CO
Lignite
Liquefaction
Oxygen content
CO consumption

ABSTRACT

This paper made a preliminary investigation of CO effects on lignite liquefaction process. The Schütze method coupled with an elemental analyzer was adopted for directly determining the O contents of liquid and solid materials, and the O balance, variation amounts of water, and CO consumptions were calculated quantitatively for liquefaction processes. It was found that the two reactions which were the water-gas shift reaction and the reaction between CO and organic structures of coals, occurred distinctly in the liquefaction process with CO atmospheres, and were simultaneously strengthened by the catalysts. The simultaneous occurrence of the two reactions played the roles of reducing the water production, elevating the coal conversion, and promoting the asphaltene (AS) and preasphaltene (PA) production.

1. Introduction

Lignite is regarded as an abundant and inexpensive resource accounting for 13% of the coal deposits in China [1]. It is a kind of preferred coals for direct liquefaction, due to its high reactivity [2–5]. However, its high oxygen and moisture contents limit its utilization in direct liquefaction, due to a large hydrogen consumption for removing O and a large energy consumption for drying [6–9]. In view of this, some researchers used syngas (or CO) and H_2O as a hydrogen source for lignite liquefaction [10–16]. Fischer et al. [10] pointed out that the use of CO and H_2O could liquefy lignite easily. Hata et al. [11] found that the coal conversion, which was basically equivalent to that in pure hydrogen, increased to 90.1% under syngas and H_2O as hydrogen source. Shui et al. [12], Subagyono et al. [13], and Guo et al. [14,15] drew a similar conclusion that the coal liquefaction activity under the system of syngas (or CO) and H_2O (or complex solvent of H_2O and organic solvent) appeared higher than that under the traditional system of H_2 and organic solvent. Our investigation [16] showed that the conversion and oil yield from Shengli lignite liquefaction under the system of syngas and complex solvent were obviously higher than those under the system of H_2 and organic solvent (especially higher production of PA). Summarily, the utilization of syngas (or CO) and H_2O as a hydrogen source is quite advantageous for lignite liquefaction. Therefore, in order to the further development and application of the lignite liquefaction technology using syngas (or CO) and H_2O as a hydrogen source, it is very imperative to make some investigations on the liquefaction process with syngas (or CO) and H_2O, especially the following issues. What are the effects (or roles) of CO and H_2O on the liquefaction process? How do the effects (or roles) of CO and H_2O occur in the liquefaction process?

This paper is only focused on the investigation of the CO effects (or roles) on the liquefaction process. From a plenty of investigations on the topic [17–24], it could be found that CO assuredly took some roles on the liquefaction process, and the roles of CO could be generally summarized as follows: a production of hydrogen from the water-gas shift reaction of CO and H_2O to provide hydrogen source for liquefaction reaction, and a more activity of produced hydrogen to stabilize free radicals in liquefaction process. Obviously, these roles of CO have been accepted universally by many researchers and scholars [18,21,25–27]. Besides the above roles, the following issues are not still known or understood. If CO takes some other effects (or roles) on liquefaction process or not? If so, what are the effects? Presently, the relevant investigations (or reports) on this topic are very scare, and only a literature [28] mentioned that CO had a probable role for directly removing O. The special investigations on this topic were not found. For this, this paper made a preliminary investigation on the lignite liquefaction process (such as the water variation after liquefaction, the distribution of liquefaction products, the O contents of liquid and solid products, and the CO consumption for liquefaction reaction, etc.) with CO atmospheres, aiming at obtaining a further understanding of the CO effects on liquefaction process.

* Corresponding authors at: Department of Chemical Engineering for Energy Resources, School of Resources and Environmental Engineering, East China University of Science and Technology, Shanghai 200237, China.

E-mail addresses: wsy@ecust.edu.cn (S. Wu), wyq@ecust.edu.cn (Y. Wu).

https://doi.org/10.1016/j.fuel.2018.02.079
Received 14 December 2017; Received in revised form 24 January 2018; Accepted 9 February 2018
Available online 24 February 2018

Nomenclature

CSARB	coal sample on as received basis
THN	tetralin
THF	tetrahydrofuran
TN	toluene
HEX	*n*-hexane
GP	gaseous product
HS	HEX-soluble fractions
W	water
HSWT	integrant for HS, THN, and W
HSW	HSWT excluding THN
AS	HEX-insoluble but TN-soluble fractions
PA	TN-insoluble but THF-soluble fractions
CT	catalysts
RSM	integrant of RS, ashes of CSARB, and CT
RS	RSM excluding ashes of CSARB and added CT (if any)
BR	reaction atmosphere before liquefaction reaction
Y	yield, %
m	mass, g
V	volume of gaseous phase in the liquefaction reactor, L
P	pressure of liquefaction reactor at 25 °C, MPa
G	concentration of j gas components in GP, %
M	molar mass of j gas components in GP, g/mol
T	water content, %
Q	variation amount of water, g/10 g CSARB
C	O contents, %
N	O mole number, mmol/10 g CSARB
TN_B	total mole number of O element in reactants, mmol/10 g CSARB
TN_A	total mole number of O element in products, mmol/10 g CSARB
R	ratio of TN_B and TN_A
E	total consumption amounts of CO mmol/10 g CSARB
E_1	consumption amount of CO from water-gas shift reaction, mmol/10 g CSARB
E_2	consumption amount of CO from the reaction of CO and coals, mmol/10 g CSARB
Z	gas mole number of j gas components, mmol/10 g CSARB
D	generation amount of j gas from the water-gas shift reaction, mmol/10 g CSARB

Subscripts

i	product (AS or PA)
j	gas components (CO, CO_2, H_2, or C_1-C_4)
k	matters (CSARB, HWST, AS, PA, or RSM)

2. Experimental

2.1. Materials

The used raw coal was a kind of lignite from Xilinhaote Coal Mine of Inner Mongolia Autonomous Region in China. The raw coal was ground to below 0.2 mm, subsequently dried at 100 °C for 12 h, and stored hermetically as coal sample on as received basis (termed as CSARB) for liquefaction experiments. The CSARB was made a proximate analysis according to the National Standard of China (GB/T 212-2008), and the contents of its moistures (M_{ar}), ashes (A_{ar}), volatile matters (V_{ar}), and fixed carbons (FC_{ar}) are 3.52%, 10.94%, 38.05%, and 47.49%, respectively. The C, H, N, S, and O contents of the CSARB, which were determined by the elemental analyzer (introduced in Section 2.3), are 61.52%, 4.13%, 1.04%, 0.40%, and 25.68%, respectively. The tetralin (THN) and Fe_3O_4 were used as solvents and catalysts for liquefaction experiments, respectively. N_2 (99.999%) and CO (99.999%) with high purity were used in liquefaction experiments. All used solvents and

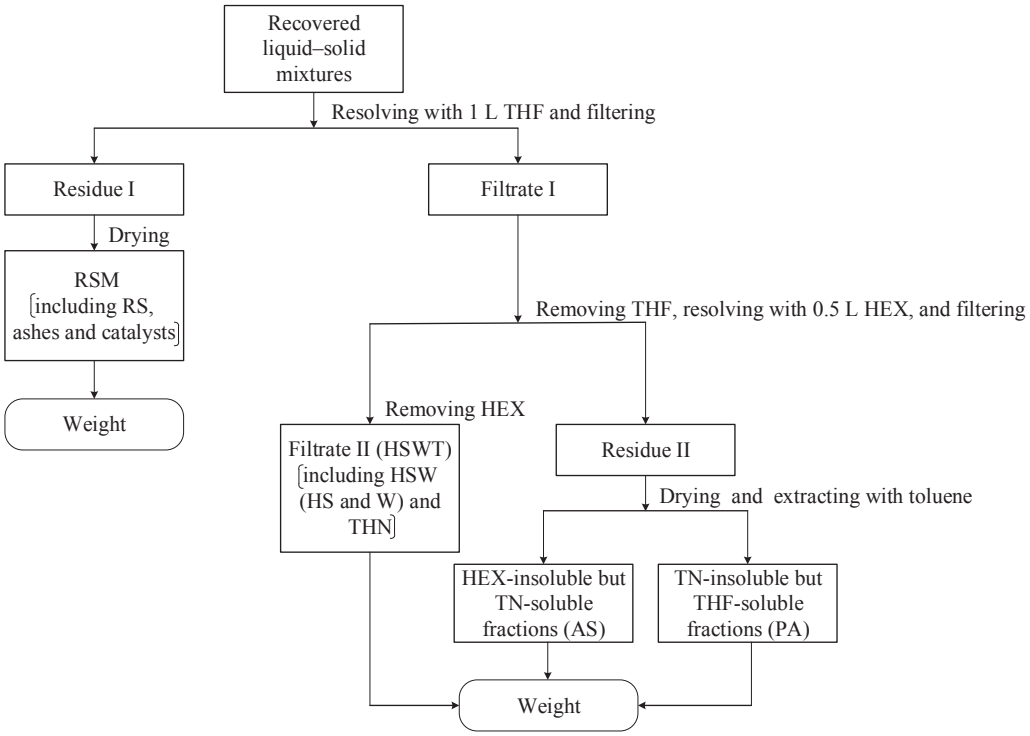

Fig. 1. Procedures for separation of recovered liquid-solid mixtures from each liquefaction experiment.

reagents including THN, tetrahydrofuran (THF), toluene (TN), and *n*-hexane (HEX) were commercially pure chemical reagents and used as received without further purification.

2.2. Liquefaction experiments and product separation

The liquefaction experiments were carried out in a 150 mL autoclave [29]. For each run, the liquefaction reactor was charged with 10.0 g CSARB, 15 mL THN, and 0.69 g Fe_3O_4 (if necessary). Subsequently, the reactor was sealed and purged by N_2 for six times before being pressurized to the desired initial pressure (4.0 MPa) of CO (or N_2), and then was heated to 430 °C. After the liquefaction process was maintained for 60 min, the reactor was quenched quickly by cooling water, and the gaseous products (GP) were collected by an aluminum foil bag for composition analysis [30].

The liquid-solid mixtures were recovered from the reactor by washing with 500 mL THF, and separated according to the procedures shown in Fig. 1. The recovered liquid-solid mixtures were resolved in 1 L THF, and then filtered to obtain Filtrate I and Residue I. Residue I after removing THF by being dried in a vacuum for 12 h was termed as RSM and collected for weight. The RSM excluding the ashes from CSARB and the added catalysts (if any) was defined as RS. Filtrate I after removing THF by rotary evaporation was resolved in 500 mL HEX, and then filtrated to obtained Filtrate II and Residue II. Filtrate II after removing HEX by rotary evaporation was termed as HSWT and collected for weight. The HSWT excluding THN was defined as HSW, and the HSW excluding water (W) was defined as HS (i.e., HEX-soluble fractions). Residue II after removing HEX by being dried in a vacuum for 12 h was separated into HEX-insoluble but TN-soluble fractions (termed as AS) and TN-insoluble but THF-soluble fractions (termed as PA) by an automatic Soxhlet extraction with TN [31,32], and the AS and PA were collected for weight, respectively.

In this paper, the two liquefaction experiments in N_2 atmospheres without and with catalysts were labelled as N_2-N and N_2-C, respectively. Likewise, those in CO without and with catalysts were labelled as CO-N and CO-C, respectively. Each liquefaction experiment was repeated at least 3 times.

2.3. Characterizations and analyses

The water content of HSWT (only 50 μL sample for determining the water content) was determined by a Karl Fischer titration analyzer (ZTWS-8A, WeiFang ZhongTe Electronic Equipment Co., Ltd.). The elemental compositions (C, H, N, and S) of CSARB were determined using an elemental analyzer (Vario MICRO Cube III (CHNS), Elementar Analysensysteme GmbH). The Schütze method [33] was adopted to directly test the O contents of liquid and solid materials (CSARB, HSWT, AS, PA, and RSM) using an elemental analyzer (Vario MACRO cube III (O), Elementar Analysensysteme GmbH) equipped with a pyrolysis tube, a CO adsorption column, and a TCD for directly detecting the O element. The determination error is 0.2%. The composition analysis of GP was conducted by a gas chromatography (GC 9790-II, Zhejiang Fu Li Analytical Instrument Co., Ltd.) equipped with a TDX-01 column (TCD for detecting H_2, CO, and CO_2) and a Plot-Al_2O_3 column (FID for detecting C_1-C_4) [34].

For the GC–MS analysis of HS (in HSWT), the HSWT after removing water was used as the testing sample. The water removal of HSWT was as follows [32]. Firstly, the HSWT was resolved by acetone to form solution. Subsequently, the solution was hydrated by Na_2SO_4 powders and filtered (simultaneously being washing by acetone for several times) to generate filtrate. Finally, the filtrate after removing acetone by rotary evaporation was used for GC–MS analysis. The GC–MS analysis was made by a GC–MS analyzer (Agilent 6890/5973N, Agilent Technologies, USA) equipped with a capillary column coated with HP-5MS (crosslink 5% PH ME siloxane, 30 m × 0.25 mm inner diameter, 0.25 μm film thickness, helium as a carrier gas at a flow rate of 1.0 mL/min, mass scanning range of 30–500 amu). The column was heated to 60 °C (holding for 2 min), and then heated to 300 °C at a rate of 5 °C/min (holding for 10 min). The organic compounds were identified by comparing the mass spectra to NIST05 and Wiley7n library data, and their relative contents (the percentage of each compound's peak area out of the total peak area excluding the peak area of THN and naphthaline) were obtained by the methods of normalization of peak areas.

3. Calculations

3.1. Yields of AS, PA, and RS

As presented in Section 2.2, the products which could be directly collected for weight in liquefaction experiments, were HSWT, AS, PA, and RSM (i.e., RS), and the HSWT contained a large quantity of solvents which could not be quantified accurately. CO and water had been involved in the liquefaction reaction as reactants, and the yields of gas and water were not suitable to be calculated. Hence, this paper only made the calculations for AS, PA, and RS yields. The yields (Y_i, %) of AS and PA for each liquefaction experiment were calculated according to Eq. (1).

$$Y_i = \frac{m_i}{m_{CSARB} \times (100\% - M_{ar} - A_{ar})} \times 100\% \quad (1)$$

where m_{CSARB} (g) and m_i (g) are the masses of CSARB and i product (i = AS or PA), respectively.

The yield (Y_{RS}, %) of RS for each liquefaction experiment was calculated according to Eq. (2).

$$Y_{RS} = \frac{m_{RSM} - m_{CT} - m_{CSARB} \times A_{ar}}{m_{CSARB} \times (100\% - M_{ar} - A_{ar})} \times 100\% \quad (2)$$

where m_{RSM} (g) and m_{CT} (g) are the mass of RSM and added catalysts, respectively. The m_{CT} is valued as 0 for the N_2-N and CO-N experiments.

3.2. Variation amounts of water for liquefaction reaction

The variation amount (Q, g/10 g CSARB) of water for each liquefaction reaction was calculated according to Eq. (3).

$$Q = \frac{(m_{HSWT} \times T_{HSWT}) - (m_{CSARB} \times M_{ar})}{m_{CSARB}/10} \quad (3)$$

where m_{HSWT} (g) is the mass of HSWT, and T_{HSWT} (%) is the water content in HSWT. The water content in HSWT for each liquefaction is

Table 1
Concentrations of various gas components in GP and water content in HSWT for each liquefaction.

Experiments	Concentrations of various gas components in GP (%)										Water content in HSWT (%)
	H_2	CO	CO_2	CH_4	C_2H_6	C_2H_4	C_3H_8	C_3H_6	C_4H_{10}	C_4H_8	
N_2-N	4.79	2.01	3.99	6.00	0.84	0.04	0.39	0.04	0.10	0.02	3.50
N_2-C	9.07	1.82	4.72	5.83	0.88	0.04	0.39	0.04	0.09	0.01	4.64
CO-N	11.58	70.19	10.86	6.22	0.68	0.04	0.31	0.03	0.08	0.01	1.07
CO-C	15.81	64.69	11.83	6.15	0.87	0.04	0.43	0.04	0.11	0.02	0.99

Table 2
The ratio between the total mole number of O element in reactants and that in all products for each liquefaction.

Experiments	TN_B (mmol/10 g CSARB)	TN_A (mmol/10 g CSARB)	R
N_2-N	160.68	169.64	0.9472
N_2-C	172.54	180.81	0.9543
CO-N	369.02	388.69	0.9494
CO-C	376.42	395.32	0.9522

listed in Table 1. The Q values below and above 0 suggest the consumption and production of water for liquefaction reaction, respectively.

3.3. O Contents of HS

Usually, the O contents of these liquids and solids (CSARB, HSWT, AS, PA, and RSM) can be calculated by difference method (i.e., 100%-the sum of C, H, N, and S contents). However, it is well-known that the organic structures of these materials are mainly made of these elements (C, H, N, S, and O), and also contain some microelements (especially coals) [35–37], such as F [38,39], Cl [40], and Br [41], etc. Thus, the O content calculated by the difference method is actually a representative of the total content of O element and these microelements, consequently resulting in a misunderstanding to the actual O content. Therefore, the O contents of CSARB, HSWT, AS, PA, and RSM in this paper were directly determinated by the elemental analyzer (introduced in Section 2.3).

As presented in Section 2.2, the HS is only a defined product, and the actual HS is separated quite difficultly from a quite large quantity of solvents presented in HSWT. Thereby, the O content of HS can not be directly obtained by the determination method introduced in Section 2.3. For this, the O content (C_{HS}, %) of HS from each liquefaction experiment was calculated according to Eq. (4).

$$C_{HS} = \frac{N_{HSWT} - \frac{T_{HSWT} \times m_{HSWT}}{18} \times 1000}{1000 \times (m_{CSARB} + m_{CT} + m_{BR} - m_{GP} - m_{AS} - m_{PA} - m_{RSM} - m_{HSWT} \times T_{HSWT})} \times 100\% \quad (4)$$

where N_{HSWT} (mmol/10 g CSARB) is the mole number of O element in HSWT, and the N_{HSWT} was calculated according to Eq. (8). m_{BR} (g) and m_{GP} (g) are the masses of reaction atmospheres and GP, respectively. The m_{BR} values for the N_2-N and N_2-C experiments were 0, and those for the CO-N and CO-C experiments were calculated according to Eq. (5). m_{GP} was calculated according to Eq. (6)

$$m_{BR} = \frac{V}{22.4} \times \frac{P}{0.101325} \times \frac{273.15}{298.15} \times 100\% \times 28 \quad (5)$$

$$m_{GP} = \frac{V}{22.4} \times \frac{P}{0.101325} \times \frac{273.15}{298.15} \times \sum (G_j \times M_j) \quad (6)$$

where G_j (%) and M_j (g/mol) are the concentration and molar mass of j gas components in GP (j = H_2, CO, CO_2, CH_4, and C_2-C_4), respectively [42]. The concentrations of various gas components in GP for each liquefaction are listed in Table 1. V (L) is the volume of gaseous phase in the liquefaction reactor, and P (MPa) is the pressure of liquefaction reactor at 25 °C.

Based on the principle of mass conservation, the O balance calculations were made for each liquefaction experiment. That is to say, the ratio (R) between the total mole number (TN_B, mmol/10 g CSARB) of O element in reactants and that (TN_A, mmol/10 g CSARB) in all products was calculated according to Eq. (7). The reactants included reaction atmosphere, CSARB, and catalysts (if any), and the products included GP, HSWT, AS, PA, and RSM.

$$R = \frac{TN_B}{TN_A} = \frac{N_{CSARB} + N_{CT} + N_{BR}}{N_{GP} + N_{HSWT} + N_{AS} + N_{PA} + N_{RSM}} \quad (7)$$

$$N_k = \frac{C_k \times m_k}{16} \times 1000/m_{CSARB} \times 10 \quad (8)$$

$$N_{GP} = \frac{V}{22.4} \times \frac{P}{0.101325} \times \frac{273.15}{298.15} \times (G_{CO} + 2G_{CO_2}) \times 1000/m_{CSARB} \times 10 \quad (9)$$

$$N_{BR} = \frac{V}{22.4} \times \frac{P}{0.101325} \times \frac{273.15}{298.15} \times 1000/m_{CSARB} \times 10 \quad (10)$$

where N_k (mmol/10 g CSARB), m_k (g), and C_k (%) are the O mole number, mass, and content of k matter (k = CSARB, HWST, AS, PA, or RSM), respectively. N_{GP} (mmol/10 g CSARB) is the O mole number of GP, G_{CO} (%) and G_{CO_2} (%) are respectively the CO and CO_2 concentrations in GP, and N_{BR} (mmol/10 g CSARB) is the O mole number of reaction atmosphere before liquefaction reaction. The N_{BR} for the N_2-N and N_2-C experiments was 0, and that for the CO-N and CO-C experiments was calculated according to Eq. (10). The N_{CT} (mmol/10 g CSARB) for the N_2-N and CO-N experiments was 0, and that for the N_2-C and CO-C experiments was calculated according to the chemical stoichiometric coefficient of catalysts (Fe_3O_4).

Table 2 gives the total mole number of O element in reactants, the total mole number of O element in all products, and the ratio of the two ones for each liquefaction. It is seen that the total mole number of O element in reactants is slightly lower than that in all products for each liquefaction, and the R values for all runs are in the range of 0.9472–0.9543. These illustrate that the above calculation of O balance is made well for each liquefaction experiment. Therefore, it is suggested that the O contents of these liquid and solid materials (CSARB, HSWT, AS, PA, and RSM) are reasonably obtained by the direct determination of the elemental analyzer (introduced in Section 2.3), and the calculated content of HS is credible.

3.4. CO consumption amounts for liquefaction reaction in CO atmosphere

The total consumption amounts of CO (E, mmol/10 g CSARB) for the CO-N and CO-C experiments were calculated quantitatively according to Eq. (11).

$$E = \frac{Z_{BR} - Z_{AR}}{m_{CSARB}} \times 10 \quad (11)$$

where Z_{BR} (mmol/10 g CSARB) is the mole number of CO in reactants and Z_{AR} (mmol/10 g CSARB) is the mole number of CO in GP. The Z_{BR} is equal to N_{BR} (Eq. (10)). The Z_{AR} is equal to Z_j (mmol/10 g CSARB) which was calculated according to Eq. (12).

$$Z_j = \frac{V}{22.4} \times \frac{P}{0.101325} \times \frac{273.15}{298.15} \times G_j \times 1000 \quad (12)$$

where Z_j is the mole number of j gas component (j = CO) in GP from each liquefaction.

Generally, it is universally accepted that the water-gas shift reaction can occur distinctly in liquefaction processes with CO atmosphere, consequently resulting in the consumption of CO [43–46]. This is also illustrated by the results of Section 4.3. For this purpose, the consumption amounts of CO for the water-gas shift reaction in the CO-N and CO-C experiments were calculated as follows. According to the stoichiometric coefficient of water-gas shift reaction, the consumption amount of CO is equal to the generation amount of CO_2 (or H_2). Hence, the generation amounts of CO_2 and H_2 from the water-gas shift reaction for the CO-N and CO-C experiments were calculated. It is well-known that CO_2 and H_2 can be generated from the coal cracking during liquefaction [47], which is also confirmed by the results of the N_2-N and N_2-C experiments (Table 1). Here, it was made an assumption that the generation amounts of CO_2 (or H_2) resulting from the coal cracking in the CO-N and CO-C experiments were equal to those of CO_2 (or H_2) resulting from the coal cracking in the N_2-N and N_2-C experiments, respectively. Consequently, the generation amounts (D_j^{CO-N}, mmol/10 g CSARB) of CO_2 (or H_2) resulting from the water-gas shift reaction in the

CO-N experiment and that (D_j^{CO-C}, mmol/10 g CSARB) in the CO-C experiment were calculated according to Eqs. (13) and (14), respectively.

$$D_j^{CO-N} = \frac{Z_j^{CO-N} - Z_j^{N_2-N}}{m_{CSARB}} \times 10 \quad (13)$$

$$D_j^{CO-C} = \frac{Z_j^{CO-C} - Z_j^{N_2-C}}{m_{CSARB}} \times 10 \quad (14)$$

where Z_j^{CO-N} (mmol/10 g CSARB) and $Z_j^{N_2-N}$ (mmol/10 g CSARB) are the mole number of j gas component (j = CO_2 or H_2) in GP from the CO-N and N_2-N experiments, respectively. Z_j^{CO-C} (mmol/10 g CSARB) and $Z_j^{N_2-C}$ (mmol/10 g CSARB) are the mole number of j gas component (j = CO_2 or H_2) in GP from the CO-C and N_2-C experiments, respectively. Z_j^{CO-N}, $Z_j^{N_2-N}$, Z_j^{CO-C}, and $Z_j^{N_2-C}$ were calculated according to Eq. (12).

Table 3 gives the generation amounts of CO_2 and H_2 resulting from the water-gas shift reaction in the CO-N and CO-C experiments. It is surprisingly found that the generation amount of CO_2 is almost equal to that of H_2 for each of the CO-N and CO-C experiments, which is coincidently in accordance with stoichiometric coefficient of water-gas shift reaction. This illustrates that the above proposed assumption is reasonable for the calculations on generation amounts of CO_2 and H_2 from water-gas shift reaction. Here, the consumption amounts (E_1, mmol/10 g CSARB) of CO from water-gas shift reaction in the CO-N and CO-C liquefaction experiments were calculated as the average value of $D_{CO_2}^{CO-N}$ and $D_{H_2}^{CO-N}$ and that of $D_{CO_2}^{CO-C}$ and $D_{H_2}^{CO-C}$, respectively.

As discussed in Section 4.3, the CO consumption for the CO-N (or CO-C) experiment was ascribed into the water-gas shift reaction and the reaction of CO and coals. Thus, the consumption amount (E_2, mmol/10 g CSARB) of CO (due to the reaction of CO and coals) for the CO-N (or CO-C) experiment was calculated as E-E_1.

4. Results and discussion

4.1. Variations of water for liquefaction reaction

Fig. 2 shows the variation amounts of water for each liquefaction. The variation amounts of water for the N_2-N and N_2-C experiments are below 0, suggesting that the water is produced in the liquefaction process with N_2 atmospheres. Meanwhile, the variation amounts of water for the CO-N and CO-C experiments are above 0, suggesting that the water is consumed in the liquefaction process with CO atmospheres. These illustrate that CO can play a role of consuming water in the liquefaction process, which has been also reported by our previous studies [16,25]. Consequently, it is suggested that the present of CO in liquefaction atmospheres is favorable for reducing the water production of the liquefaction process. It was reported by literatures [48–50] that the consumption of water was mainly ascribed into the water-gas shift reaction occurring in the liquefaction process, which was in accordance with the result (an obvious CO consumption amount (E_1) ascribed into the water-gas shift reaction) in Section 4.3.

Many literatures [46,51–54] have reported that the catalysts with Fe active component. From this consideration, the consumption amount of water for the CO-C experiment should be distinctly larger than that for the CO-N experiment. However, it is found that the consumption amount of water for the former is slightly larger than that for the latter, which is in accordance with the result (the consumption amount of CO (E_1) for the former is slightly larger than that (E_1) for the latter) in Section 4.3. This is probably due to the Fe-containing reactor wall, which also can take a catalytic role on the water-gas shift reaction. In a word, it can be convinced that the consumption amount of water for the CO-C experiment is assuredly larger than that for the CO-N experiment. Therefore, it is concluded that the addition of the Fe_3O_4 catalysts can result in reducing the water production of liquefaction process with CO atmospheres, owing to promoting the water-gas shift reaction.

4.2. O Contents of HS, AS, PA, and RSM

Fig. 3 shows the O contents of HS, AS, PA, and RSM for each liquefaction experiment. It can be seen that the O contents of HS for all liquefaction experiments are up to 29.31–43.61%, obviously suggesting that the HS is abundant in O element and presents oxygen-rich species. Here, the HS (from the CO-C experiment) as a typical representative, was analyzed by the GC–MS analyzer (introduced in Section 2.3). The compositions of the HS can be roughly divided into two classifications: oxygen-containing compounds and oxygen-free compounds, and the relative contents of various oxygen-containing compounds are listed in Table 4. According to Table 4, the oxygen-containing compounds were classified and shown in Fig. 4. It is found that the oxygen-containing compounds are alcohols, phenols, ethers, ketones, and esters, and their total content is up to 15.83%. These results suggest that the HS contains abundant oxygen-containing structures such as phenolic hydroxyls, alcoholic hydroxyls, ether groups, carbonyl groups, and ester groups [55].

As presented in Fig. 3, the respective O contents of HS and RSM from the CO-N experiment are higher than those from the N_2-N experiment, and the respective O contents of PA and AS from the CO-N experiment are slightly higher than those from the N_2-N experiment. Simultaneously, the above similar phenomena are also presented in the liquefaction experiments with catalyst (i.e., the N_2-C and CO-C experiments). These results illustrate that the O of CO probably enters into coals, consequently resulting in the increasing O contents of HS, AS, PA, and RSM. Thereby, it can be inferred that CO probably reacts with organic structures of coals during liquefaction.

In addition, the respective O contents of HS, AS, PA, and RSM from the CO-C experiment are higher than those from the CO-N experiment, consequently suggesting that the addition of catalysts can result in the increasing O contents of HS, AS, PA, and RSM from the liquefaction process with CO atmospheres. This illustrates that the catalysts promote the reaction between CO and organic structures of coals during liquefaction, but the extra O in RSM is from the catalyst (Fe_3O_4). To sum up, it can be qualitatively inferred that the reaction between CO and organic structures of coals occurs probably during liquefaction and can be further promoted by the catalysts.

4.3. CO consumption for liquefaction reaction in CO atmospheres

In order to further understand and illustrate the results of Sections 4.1–4.2, the consumption amount (E_1) of CO (consumed by the water-gas shift reaction), that (E_2) of CO (consumed by the reaction between CO and organic structures of coals), and the total consumption (E) of CO (the sum of the above two ones) for the CO-N and CO-C experiments were respectively calculated, and the results are presented in Fig. 5. The E values for the CO-N and CO-C experiments illustrate that CO is obviously consumed in the liquefaction process with CO atmospheres, and the E_1 and E_2 values for the above two experiments illustrate that both of the two reactions (water-gas shift reaction and the reaction between CO and organic structures of coals) occur distinctly in the liquefaction process with CO atmospheres. Besides, the comparison between E_1 and E_2 values of the CO-N and CO-C experiments illustrate that the catalysts can play a promotion role on both of the two reactions (water-gas shift reaction and the reaction between CO and organic structures of coals). The above results quantitatively confirm the conclusion of Section 4.1 and the inference of Section 4.2. Therefore, it is drawn a conclusion that

Table 3
Generation amounts of CO_2 and H_2 resulting from the water-gas shift reaction in the CO-N and CO-C experiments.

Experiments	D_{H_2} (mmol/10 g CSARB)	D_{CO_2} (mmol/10 g CSARB)
CO-N	17.41	17.62
CO-C	18.47	19.02

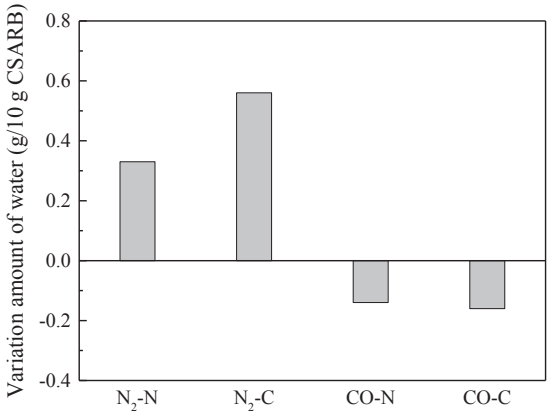

Fig. 2. Variation amounts of water for each liquefaction.

in the liquefaction process with CO atmospheres, the water-gas shift reaction and the reaction between CO and organic structures of coals are dominantly presented and can be simultaneously promoted by the catalysts.

Presently, there are no special investigations on the reaction between CO and organic structures of coals in the liquefaction systems, and only a literature [28] proposed a relevant viewpoint that CO probably reacted with oxygen-containing structures of coals to directly remove oxygen. However, this viewpoint is not in accordance with the results (the presence of CO results in the increasing O contents of HS, AS, PA, and RSM) of Section 4.2. Hence, it can be said that the mechanisms for this reaction are ambiguous and even unclear. For this, there is a strong need to investigate the mechanisms for this reaction, and this investigation will be regarded as a very important topic for being successively studied in the future.

4.4. Yields of AS, PA, and RS

Fig. 6 shows the yields of RS, PA, and AS for each liquefaction. The yields of RS for the CO-N and CO-C experiments are respectively lower

Table 4
Relative contents of oxygen-containing compounds in HS for the CO-C experiment.

No.	Compounds	Formula	RC[a]
Alcohols			
1	Benzenemethanol	C_7H_8O	0.79
2	2-Methyl-1-phenyl-1-propanol	$C_{10}H_{14}O$	2.17
3	1,5-diphenylpent-2-yne-1,5-diol	$C_{17}H_{16}O_2$	0.57
4	1.2-Phenyl-2-pentanol	$C_{11}H_{16}O$	2.60
5	4,5-trimethyl-Benzenemethanol	$C_{10}H_{14}O$	0.36
6	Hexadecanol-2	$C_{16}H_{34}O$	0.51
7	MTHTDBAPO[b]	$C_{20}H_{28}O_6$	0.13
Phenols			
8	Phenol	C_6H_6O	0.59
9	3,4-dimethyl-Phenol	$C_8H_{10}O$	1.37
10	2-ethyl-5-methyl-Phenol	$C_9H_{12}O$	0.38
11	5-Hydroxyhydrindene	$C_9H_{10}O$	1.99
12	Dibenzosuberol	$C_{15}H_{14}O$	0.57
Ethers			
13	DPDO[b]	$C_{16}H_{16}O_2$	0.16
14	EPDYE[b]	$C_{28}H_{44}O_4$	0.88
Ketones			
15	TEDD[b]	$C_{20}H_{18}O_2$	0.41
16	NEMDHCYENM[b]	$C_{20}H_{24}N_2O$	0.48
17	bis(2-vinylphenyl)methanone	$C_{17}H_{14}O$	0.13
18	DYHDDHCAO[b]	$C_{28}H_{42}O_2$	0.87
Esters			
19	2-(azulen-1-yl)ethyl acetate	$C_{14}H_{14}O_2$	0.88

[a] The relative content (%) is defined as the percentage of each compound's chromatographic area out of the total peak area (only those compounds with relative content of above 0.1% are listed).

[b] Abbreviation of compound names (MTHTDBAPO: 2-methyl-1-(1a,2,3a,5-tetrahydroxy-7 (hydroxymethyl)-1,1,3-trimethyl-1,1a,2,3,3a,4,5,6,8a,8b-decahydrocyclopropa[3,4]benzo[1,2] [7]annulen-5-yl)propan-1-one; DPDO: 3,3-dimethyl-1-phenyl-1,3-dihydroisobenzofuran-1-ol; EPDYE: (E)-2-phenyl-1,3-dioxolan-4-yl octadec-9-enoate; TEDD: 1,1′-(4a,9,9a,10-tetrahydro-9, 10-ethanoanthracene-11,12-diyl)diethanone; NEMDHCYENM: N-(2-(3-ethyl-1-methyl-9,9a- dihydro-4aH-carbazol-2-yl)ethyl)-N-methylacetamide; DYHDDHCAO: 3-(5,6-dimethylheptan -2-yl-11b-hydroxy-3a,6-dimethyl-2,3,3a,4,5,7,8,9,10,11b-decahydro-1H-cyclopenta[a] anthracen-1-one.

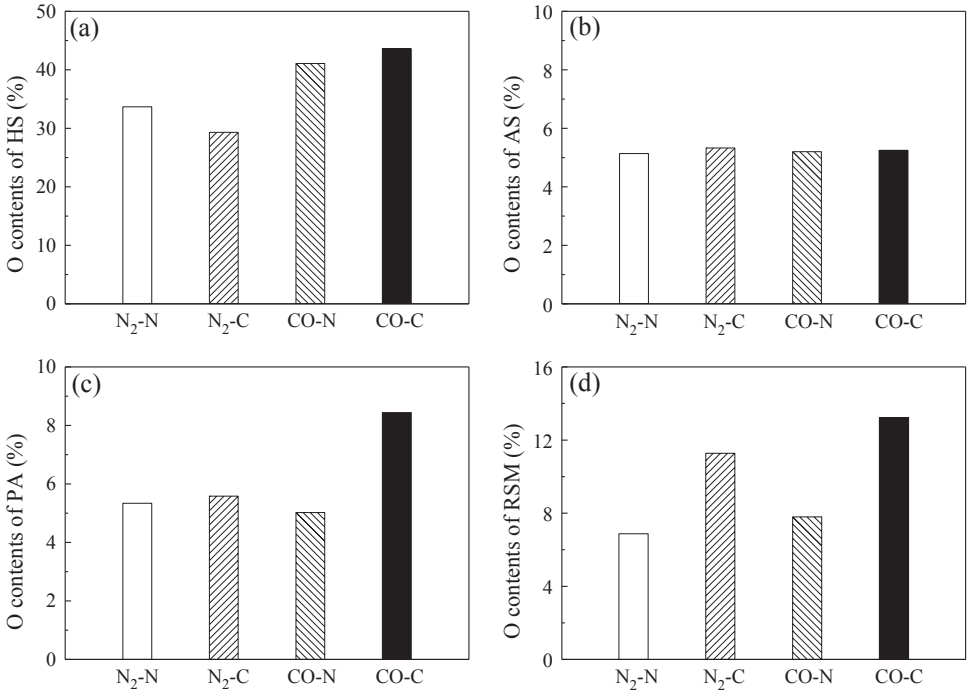

Fig. 3. O contents of HS, AS, PA, and RSM for each liquefaction.

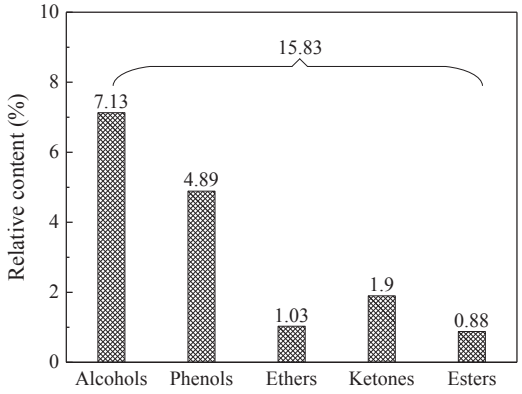

Fig. 4. Distributions of oxygen-containing compounds in HS from the CO-C experiment.

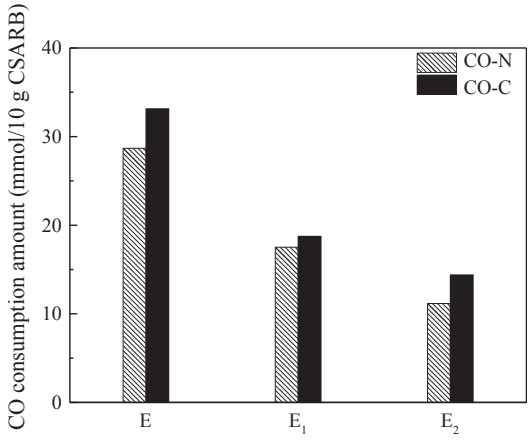

Fig. 5. CO consumption amounts for the liquefaction with CO atmospheres.

than those for the N_2-N and N_2-C experiments, suggesting that the presence of CO in liquefaction atmospheres results in the increasing conversion of coals. The respective yields of AS and PA for the CO-N and CO-C experiments are respectively higher than those for the N_2-N and N_2-C experiments, suggesting that the presence of CO in liquefaction atmospheres promotes the production of both AS and PA. These illustrate that CO plays a role of promoting the coal conversion to AS and PA in the liquefaction process. Meanwhile, the respective yields of AS and PA for the CO-C experiment are distinctly higher than those for the CO-N experiment, suggesting that the addition of catalysts strengthens the CO promotion role of the coal conversion to AS and PA in the liquefaction process with CO atmospheres. Summarily, it is concluded that CO plays a role of promoting the coal conversion in the liquefaction process with CO atmospheres and the promotion role of CO can be strengthened by the catalysts. Obviously, the above results are probably ascribed into the combination of the two reactions occurring during liquefaction process with CO atmospheres: promoting the coal cracking by the reaction between CO and organic structures of coals (Sections 4.2–4.3), and providing the active hydrogen by the water-gas shift reaction (Section 4.1) to stabilize free radicals from the coal cracking [17,56].

5. Conclusions

The Schütze method coupled with the elemental analyzer was credible and convenient for directly determining the O contents of liquid and solid materials (such as CSARB, HSWT, AS, PA, and RSM). Thus, the O balance calculation for each liquefaction could be made well. The presence of CO in liquefaction atmospheres took the following effects on liquefaction process: reducing the water production, elevating the O contents of HS, AS, PA, and RSM, and promoting the conversion of coals and the productions of AS and PA. Meanwhile, the addition of catalysts could strengthen the above effects. It was inferred that the above effects were mainly ascribed into the two reactions occurring during the liquefaction process with CO atmospheres (the water-gas shift reaction and the reaction between CO and organic structures of coals). Presently, the mechanisms for the reaction between CO and organic structures of coals were ambiguous and even unclear. Summarily, besides the water-gas shift reaction, the reaction of CO and organic structures of coals could play a promotion role on the liquefaction process with CO-containing atmospheres.

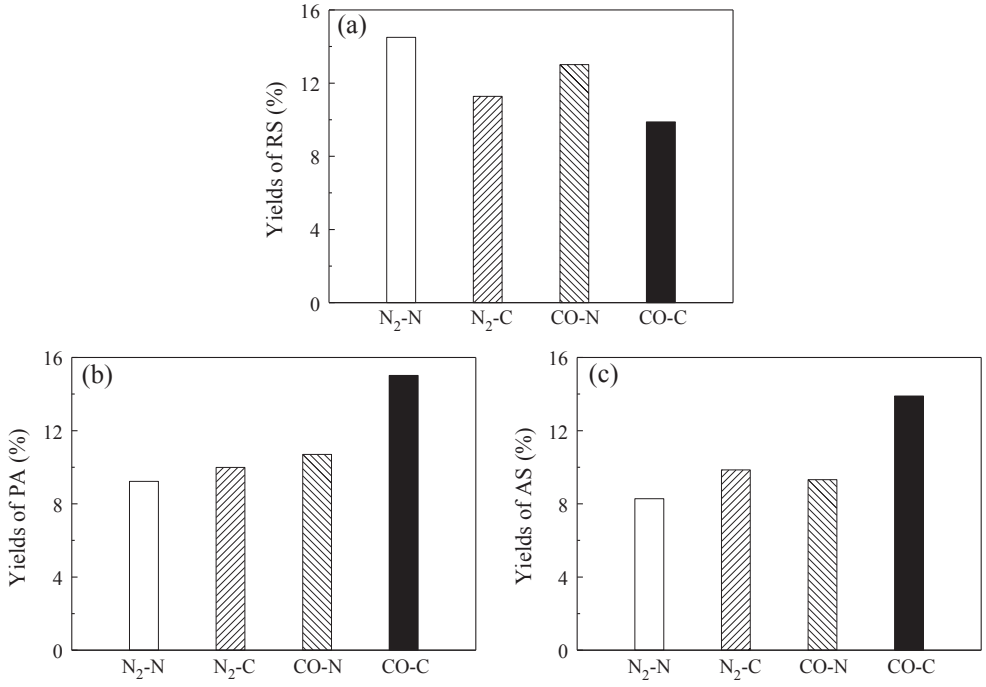

Fig. 6. The conversion and yields of RS, PA, and AS for each liquefaction.

Acknowledgements

This work was supported by the National Natural Science Foundation of China (grants 21476079 and 21476080), the Fundamental Research Funds for the Central Universities (grant WB1414014).

References

[1] Miao Z, Tian J, He Q, Wan K, Zhou G, Ren X, et al. Drying kinetics of soft and hard lignite and the surface characteristics of products. Energy Fuels 2017;31:2439–47.
[2] Artanto Y, Jackson WR, Redlich PJ, Marshall M. Liquefaction studies of some Indonesian low rank coals. Fuel 2000;79:1333–40.
[3] Lei Z, Liu M, Gao L, Shui H, Wang Z, Ren S. Liquefaction of Shengli lignite with methanol and CaO under low pressure. Energy 2011;36:3058–62.
[4] Lei Z, Liu M, Shui H, Wang Z, Wei X. Study on the liquefaction of Shengli lignite with NaOH/methanol. Fuel Process Technol 2010;91:783–8.
[5] Liu F, Wei X, Fan M, Zong Z. Separation and structural characterization of the value-added chemicals from mild degradation of lignites: a review. Appl Energy 2016;170:415–36.
[6] Miknis FP, Netzel DA, Turner TF, Wallace JC, Butcher CH. Effect of different drying methods on coal structure and reactivity toward liquefaction. Energy Fuels 1996;10:631–40.
[7] Mochida I, Okuma O, Yoon SH. Chemicals from direct coal liquefaction. Chem Rev 2014;114:1637–72.
[8] Shui H, Cai Z, Xu C. Recent advances in direct coal liquefaction. Energies 2010;3:155–70.
[9] Liu Z, Shi S, Li Y. Coal liquefaction technologies—Development in China and challenges in chemical reaction engineering. Chem Eng Sci 2010;65:12–7.
[10] Fisher F, Schrader H. The origin and chemical structure of coal. Brennstoff Chem 1921;2:37–45.
[11] Hata KA, Watanabe Y, Wada K, Mitsudo TA. Iron sulfate/sulfur-catalyzed liquefaction of Wandoan coal using syngas–water as a hydrogen source. Fuel Process Technol 1998;56:291–304.
[12] Shui H, Liu J, Wang Z, Zhang D. Preliminary study on liquefaction properties of Xiaolongtan lignite under different atmospheres. J Fuel Chem Technol 2009;37:257–61.
[13] Subagyono DJN, Marshall M, Jackson WR, Chaffee AL. Improvement in liquid fuel product quality from reactions of grape marc with CO/H_2O. Fuel 2015;159:234–40.
[14] Guo Z, Bai Z, Bai J, Wang Z, Li W. Co-liquefaction of lignite and sawdust under syngas. Fuel Process Technol 2011;92:119–25.
[15] Guo Z, Bai Z, Bai J, Wang Z, Li W. Synergistic effects during co-pyrolysis and liquefaction of biomass and lignite under syngas. J Therm Anal Calorim 2015;119:2133–40.
[16] Li Q, Chen Z, Zhou Q, Li D, Li L, Wu S. Shengli lignite liquefaction under syngas and complex solvent. J Fuel Chem Technol 2016;44:257–62.
[17] Takemura Y, Ouchi K. Catalytic liquefaction of various coals using a mixture of carbon monoxide and water. Fuel 1983;62:1133–7.
[18] Niu B, Jin L, Li Y, Hu H. Isotope analysis for understanding the hydrogen transfer mechanism in direct liquefaction of Bulianta coal. Fuel 2017;203:82–9.
[19] Hodges S, Creasy DE. The effect of alkali metal carbonate catalysts on the liquefaction of victorian brown coal using carbon monoxide and steam. Fuel 1985;64:1229–34.
[20] Vasireddy S, Morreale B, Cugini A, Song C, Spivey JJ. Clean liquid fuels from direct coal liquefaction: chemistry, catalysis, technological status and challenges. Energy Environ Sci 2011;4:311–45.
[21] Bianco AD, Piero GD, Serenellini S. Conversion of coal in CO/H_2O base system: interaction between water-gas shift reaction catalysts and coal mineral matter. Fuel 1988;67:874–5.
[22] Sondreal EA, Wilson WG, Stenberg VI. Mechanisms leading to process improvements in lignite liquefaction using CO and H_2S. Fuel 1982;61:925–38.
[23] Onsan I. Catalytic processes for clean hydrogen production from hydrocarbons. Turk J Chem 2007;31:531–50.
[24] Nandi BN, Macphee JA, Ciavaglia LA, Chornet E, Arsenault R. Enhancement of plastic properties of inert-rich oxidized cretaceous coals via the water-gas shift reaction. Fuel 1987;66:473–8.
[25] Avşar E. Dimensionality reduction for predicting CO conversion in water gas shift reaction over Pt-based catalysts using support vector regression models. Int J Hydrogen Energy 2017;42:23326–33.
[26] Odabaşi Ç, Günay ME, Yildirim R. Knowledge extraction for water gas shift reaction over noble metal catalysts from publications in the literature between 2002 and 2012. Int J Hydrogen Energy 2014;39:5733–46.
[27] Shoko E, Mclellan B, Dicks AL, Costa JCDD. Hydrogen from coal: production and utilisation technologies. Int J Coal Geol 2006;65:213–22.
[28] Wu C, Xie K. Direct coal liquefaction. Beijing: Chemical Industry Press; 2010. p. 60.
[29] Huang H, Yuan X, Zhu H, Li H, Liu Y, Wang X, et al. Comparative studies of thermochemical liquefaction characteristics of microalgae, lignocellulosic biomass and sewage sludge. Energy 2013;56:52–60.
[30] Li L, Huang S, Wu S, Wu Y, Gao J. Roles of Na_2CO_3 in lignite hydroliquefaction with Fe-based catalyst. Fuel Process Technol 2015;138:109–15.
[31] Castro LD, Priego-Capote F. Soxhlet extraction: past and present panacea. J Chromatogr A 2010;1217:2383–9.
[32] You Q, Wu S, Wu Y, Huang S, Gao J, Shang J, et al. Product distributions and characterizations for integrated mild-liquefaction and carbonization of low rank coals. Fuel process Technol 2017;156:54–61.
[33] Montgomery WJ. Analytical methods for coal and coal products. Ottawa: Academic Press; 1978. p. 217.
[34] Li L, You Q, Wu S, Huang S, Wu Y, Gao J. Co-liquefaction behavior of corn straw and Shengli lignite. J Energy Inst 2016;89:335–45.
[35] Tu H, Li W, Bai X. Distribution of phosphorus in Chinese coal. J Fuel Chem Technol 2011;39:641–6.
[36] Shi W, Dai X, Bai J, Kong L, Xu J, Li X, et al. A new method of estimating the liquidus temperature of coal ash slag using ash composition. Chem Eng Sci 2018;175:278–85.
[37] Yan T, Kong L, Bai J, Bai Z, Li W. Thermomechanical analysis of coal ash fusion behavior. Chem Eng Sci 2016;147:74–82.
[38] Xie P, Guo W, Yan X, Xue Z. Fluorine in Lopingian superhigh-organic-sulfur coals from the Lalang Coal Mine, Guangxi, southern China. Fuel 2017;208:483–90.
[39] Dai S, Ren D. Fluorine concentration of coals in China—An estimation considering coal reserves. Fuel 2006;85:929–35.
[40] Frigge L, Ströhle J, Epple B. Release of sulfur and chlorine gas species during coal combustion and pyrolysis in an entrained flow reactor. Fuel 2017;201:105–10.
[41] Saha D, Chakravarty S, Shome D, Basariya MR, Kumari A, Kundu AK, et al. Distribution and affinity of trace elements in Samaleswari coal, Eastern India. Fuel 2016;181:376–88.
[42] Kaneko T, Tazawa K, Okuyama N, Tamura M, Shimasaki K. Effect of highly dispersed iron catalyst on direct liquefaction of coal. Fuel 2000;79:263–71.
[43] Sato T, Kurosawa Jr S, RS, Adschiri T, Arai K. Water gas shift reaction kinetics under noncatalytic conditions in supercritical water. J Supercrit Fluid 2004;29:113–9.
[44] Chem WH, Tsai CW, Lin YL, Chein RY, Yu CT. Reaction phenomena of high-temperature water gas shift reaction in a membrane reactor. Fuel 2017;199:358–71.
[45] Gradisher L, Dutcher B, Fan M. Catalytic hydrogen production from fossil fuels via the water gas shift reaction. Appl Energy 2015;139:335–49.
[46] Meshkani F, Rezaei M. Preparation of mesoporous nanocrystalline iron based catalysts for high temperature water gas shift reaction: effect of preparation factors. Chem Eng J 2015;260:107–16.
[47] Mráziková J, Sindler S, Veverka L, Macák J. Evolution of organic oxygen bonds during pyrolysis of coal. Fuel 1986;65:342–5.
[48] Arab A, Sharafie D, Fazli M. Theoretical study of water-gas shift reaction on the silver nanocluster. J Phys Chem Solids 2017;109:100–8.
[49] Levalley TL, Richard AR, Fan M. The progress in water gas shift and steam reforming hydrogen production technologies-A review. Int J Hydrogen Energy 2014;39:16983–7000.
[50] Rubin K, Pohar A, Dasireddy VDBC, Likozar B. Synthesis, characterization and activity of CuZuGaOx catalysts for the water-gas shift (WGS) reaction for H_2 production and CO removal after reforming. Fuel Process Technol 2018;169:217–25.
[51] Zhu M, Rocha TCR, Lunkenbein T, Knopgericke A, Schlögl R, Wachs IE. Promotion mechanisms of iron oxide-based high temperature water-gas shift catalysts by chromium and copper. ACS Catal 2016;6:4455–64.
[52] Zhu M, Wachs IE. Iron-based catalysts for the high-temperature water-gas shift (HT-WGS) reaction: a review. ACS Catal 2016;6:722–32.
[53] Patlolla A, Carino EV, Ehrlich SN, Stavitski E, Frenkel AI. Application of operando XAS, XRD, and Raman spectroscopy for phase speciation in water gas shift reaction catalysts. Acs Catal 2012;2:2216–23.
[54] Reddy GK, Gunasekara K, Boolchand P, Smirniotis PG. Cr- and Ce-doped ferrite catalysts for the high temperature water-gas shift reaction: TPR and mossbauer spectroscopic study. J Phys Chem C 2011;115:920–30.
[55] Rizkiana J, Guan G, Widayatno WB, Hao X, Wang Z, Zhang Z, et al. Oil production from mild pyrolysis of low-rank coal in molten salts media. Appl Energy 2015;154:944–50.
[56] Wang T, Wang H, Meng X, Meng B, Tan X, Sunarso J, et al. Enhanced hydrogen permeability and reverse water-gas shift reaction activity via magneli Ti_4O_7 doping into$SrCe_{0.9}Y_{0.1}O_{3-\delta}$ hollow fiber membrane. Int J Hydrogen Energy 2017;42:12301–9.